Chromatic discrimination: differential contributions from two adapting fields

Dingcai Cao* and Yolanda H. Lu

Department of Ophthalmology and Visual Sciences, University of Illinois at Chicago, 1905 West Taylor Street, Room 149, Chicago, Illinois 60615, USA
**Corresponding author: dcao98@uic.edu*

Received August 3, 2011; revised October 10, 2011; accepted October 17, 2011; posted October 17, 2011 (Doc. ID 152292); published November 15, 2011

To test whether a retinal or cortical mechanism sums contributions from two adapting fields to chromatic discrimination, L/M discrimination was measured with a test annulus surrounded by an inner circular field and an outer rectangular field. A retinal summation mechanism predicted that the discrimination pattern would not change with a change in the fixation location. Therefore, the fixation was set either in the inner or the outer field in two experiments. When one of the adapting fields was "red" and the other was "green," the adapting field where the observer fixated always had a stronger influence on chromatic discrimination. However, when one adapting field was "white" and the other was red or green, the white field always weighted more heavily than the other adapting field in determining discrimination thresholds, whether the white field or the fixation was in the inner or outer adapting field. These results suggest that a cortical mechanism determines the relative contributions from different adapting fields.

OCIS codes: 330.1690, 330.4060, 330.5510, 330.7320.

1. INTRODUCTION

Chromatic discrimination refers to our ability to discriminate two equiluminant lights based solely on a chromaticity difference. Modern studies measure chromatic discrimination with chromaticities specified within an equiluminant cone chromaticity space, such as the MacLeod and Boynton cone chromaticity diagram [1], and with stimuli varying along the two cardinal axes, one representing L- relative to M-cone excitation and the other representing S-cone excitation. Therefore, chromatic discrimination can be further classified as L/M discrimination or S discrimination [2–5]. In the presence of one adapting field, chromatic discrimination is best at the adapting chromaticity and then deteriorates with increasing chromatic contrast between the test and adapting fields [4,6]. Such chromatic discrimination data have been explained by a model based on primate ganglion cell responses in the parvocellular (PC) and koniocellular (KC) pathways [4,5,7].

Chromatic discrimination in the presence of two or more adapting fields has not been extensively explored. Indeed, only a few studies have used more complex visual stimuli for chromatic discrimination. For instance, Zaidi *et al.* [8] measured L/M discrimination after adapting to a textured chromatic adapting field that consisted of "red" and "green" patches. They found multiple minima in their discrimination thresholds (which produced an approximately W-shaped function). Their results could not be explained by adaptation to the spatial average of the chromaticities in the textured field, an expected outcome from eye movements [9]. Instead, a worst detector model that included three independent detection mechanisms, adapting red, green, and "white," could explain their findings. Other studies using variegated adapting fields also demonstrated differential results from studies using one adapting field [10–12].

In this study, we measured L/M discrimination in the presence of two adapting fields, one inside and the other outside an annular test field. Compared with variegated stimuli, the two adapting fields in our stimulus configuration did not have direct contact. This simpler design enabled us to avoid potential interactions between the two adapting fields that may affect chromatic discrimination in a complex way. We carried out two experiments, the first with the fixation located in the inner adapting field and the second with the fixation in the outer field. The rationale was that if retinal mechanisms, such as spatial averaging from eye movements, determined relative contributions from the two adapting fields, changing the fixation location would not change the pattern of chromatic discrimination thresholds, assuming the pattern of fixational eye movement would not change dramatically. Therefore, our design allowed us to investigate the neural locus for combining the contributions from the two adapting fields that influenced chromatic discrimination. The results showed that if none of the adapting fields appeared white, the adapting field where fixation was located influenced chromatic discrimination more than the other field, suggesting that a cortical mechanism plays a major role in determining the relative contributions from the two adapting fields. We further implemented two physiologically plausible models for chromatic discrimination in the presence of two adapting fields. The first model assumed that the spectral opponency signal used for chromatic discrimination was generated by the test cone excitations and the weighted average of cone excitations from the two adapting fields. The second model assumed that the spectral opponency was generated separately between the test and each of the two adapting fields, with the resulting opponency signals subsequently combined to determine chromatic discrimination. We found that only the second model could adequately describe the chromatic discrimination data.

Because summation of two spectral opponency signals cannot occur at a retinal site, our modeling results also suggested the involvement of a cortical mechanism in determining chromatic discrimination in the presence of two adapting fields.

2. OBSERVERS

The two authors, DC (male, age 41 years) and YL (female, age 25 years), participated in the study. Both have normal color vision (assessed by the Neitz OT anomaloscope) and hue discrimination (assessed by the Farnsworth-Munsell 100-hue test). Observer YL was unaware of the purpose and design of the experiment at the time of the data collection. All experimental procedures were approved by the University of Chicago Institutional Review Board.

3. EQUIPMENT

The stimuli were generated using an iMac computer with a 10 bit video card to control a 17 in. NEC CRT color monitor at a refresh rate of 75 Hz. The CRT was well calibrated by measuring the spectral outputs of the red, green, and blue guns of the CRT using a Photo Research PR-650 spectrophotometer. The linearity of each gun was established by measuring the light outputs at 1024 light levels. With one step change in each gun, the 10 bit video card could provide resolution at a 0.0004 level in L/(L + M) chromaticity, sufficient for measuring L/M chromatic discrimination [4,13].

4. STIMULI

The spatial configuration (Fig. 1) included a 2° wide annulus surrounded by a circular inner (12° in diameter) and an outer rectangular (full size of the CRT monitor) adapting field. A black cross (0.14°) served as the fixation point, set in the center of the inner field for experiment 1 or 6° from the outer edge of the test patch in the outer field for experiment 2. Therefore, in both experiments, the fixation target was at the same distance from the center of the test patch (7°). A fan-shaped test patch with a central angle of 0.056π sat on the annulus, crossing the horizontal axis of the stimuli.

The luminance of the stimuli was 18.37 cd/m^2 (162.2 effective trolands [14]). Heterochromatic flicker photometry (12.5 Hz) was used to establish equiluminance for each observer. Stimulus chromaticities were defined in a relative cone troland space [15], in which an equal-energy-spectrum light had a chromaticity of L/(L + M) = 0.665 and S/(L + M) = 1.0. The S/(L + M) chromaticity for all stimuli was set to be 1.0. The L/(L + M) chromaticities of the adapting fields were 0.64 (green), 0.665 (white), or 0.70 (red), leading to six inner–outer adapting field combinations (red–green, green–red, red–white, white–red green–white and white–green). The L/(L + M) chromaticity of the test annulus included the chromaticities of the adapting field (0.64, 0.665, and 0.70), as well as the average of any two of the adapting field chromaticities: 0.653 (the average of 0.64 and 0.665), 0.67 (the average of 0.64 and 0.70), and 0.683 (the average of 0.665 and 0.70). Control experiments included equivalent chromaticities in both adapting fields (i.e., red–red, white–white and green–green pairs).

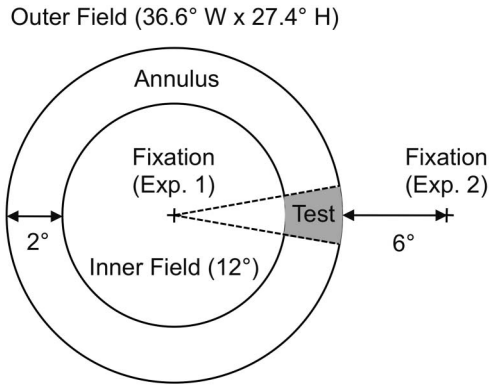

Fig. 1. Spatial configuration of the stimulus. A 12°–16° annulus was surrounded by an inner circular field and an outer rectangular field. A "+" (0.14°) served as the fixation, which was located in the center of the inner field in experiment 1 or 6° away from the annulus for experiment 2. In both experiments, the fixation had the same distance (7°) from a fan-shaped test patch center. The test patch was a section of the annulus with a central angle of 0.056π.

5. L/M CHROMATIC DISCRIMINATION MODELS

A. Model for One Adapting Field

A primate PC-ganglion cell based model has been developed to account for L/M chromatic discrimination in the presence of one adapting field [4,7,13]. The model includes a first-stage gain control mechanism and a second-stage spectrally opponent signal, which is subject to subtractive feedback. The response to a chromatic contrast change from the adapting chromaticity follows a static saturation function for a PC contrast response. The mathematical details of the model are described next.

For a test light (in our case, the light in the annulus, Fig. 1) with L- and M-cone trolands of L_T and M_T and an adapting light with cone trolands of L_A and M_A, the L- and M-cone responses, R_{LT} and R_{MT}, are determined by the test cone trolands and a gain control mechanism based on adapting cone trolands:

$$R_{L_T} = (L_T/l_{\max})G(L_A), \tag{1}$$

$$R_{M_T} = (M_T/m_{\max})G(M_A), \tag{2}$$

where $l_{\max}(= 0.63721)$ and $m_{\max}(= 0.39242)$ are maximal sensitivities of the Smith and Pokorny [16] cone fundamentals and $G(L_A)$ and $G(M_A)$ are gain functions. That is, $G(L_A) = 1/(1 + 0.33L_A/l_{\max})^{0.5}$ and $G(M_A) = 1/(1 + 0.33M_A/m_{\max})^{0.5}$.

The cone spectral opponent term can be derived for each of the subtypes of PC-pathway cell, (+L/ − M), (+M/ − L), (−L/ + M), and (−M/ + L). For a (+L/ − M) cell, for example, the spectral term at the test chromaticity is given by

$$\begin{aligned} OPP_{(+L/-M)} &= [R_{L_T} - k_1 R_{M_T}] \\ &= [L_T/l_{\max}G(L_A) - k_1 M_T/m_{\max}G(M_A)], \end{aligned} \tag{3}$$

where k_1 represents the spectral opponency surround strength. In retinal ganglion cells, the surround strength of PC-pathway cells is in the range of 0.7–1.0 [17] and 0.8 is used for the PC modeling. For equiluminant chromatic stimuli, the (+L/ − M) and (−M/ + L) give redundant information, responding positively to "redward" changes from their adaptation point; similarly, the (+M/ − L) and (−L/ + M) give redundant information, responding positively to "greenward"

changes from their adaptation point [18]. To model the PC spectral response, only a pair of cells of opposite chromatic signatures is required; for example, (+L/ – M) for a redward response and (+M/ – L) for a greenward response.

The spectral opponency signals are subject to a subtractive feedback, which is determined by the strength of the opponent signal at the adapting chromaticity:

$$OPP_C = OPP_T - k_2 OPP_A, \tag{4}$$

where OPP_C is the spectral opponent signal to a chromaticity change, C, from a fixed adapting chromaticity, A, to a test chromaticity, T. OPP_T is the spectral opponent term at the test chromaticity, OPP_A represents the spectral opponent term at adapting chromaticity, k_2 represents the subtractive feedback strength, and 0.95 is used for the model. If $C = 0$ (i.e., the test and adapting chromaticity are equal), then OPP_T is substituted by OPP_A in Eq. (4). The response of a spectral opponent cell to a chromaticity change, C, from a fixed adapting chromaticity, A, is

$$R_{OPP} = R_{\max} \cdot OPP_C/(OPP_C + SAT), \tag{5}$$

where OPP_C is a spectral opponent term in Eq. (4), $R_{\max}$ is the maximum response, and SAT is the static saturation. For a (+L/ – M) cell, the spectral opponency is

$$\begin{aligned} OPP_{C_{+L/-M}} = {} & [L_T/l_{\max}G(L_A) - k_1 M_T/m_{\max}G(M_A)] \\ & - k_2[L_A/l_{\max}G(L_A) - k_1 M_A/m_{\max}G(M_A)]. \end{aligned} \tag{6}$$

The spectral response of a (+L/ – M) cell will be

$$R_{OPP_{+L/-M}} = R_{\max} \cdot OPP_{C_{+L/-M}}/(OPP_{C_{+L/-M}} + SAT). \tag{7}$$

Given a criterion for discrimination, δ, the threshold of chromatic discrimination based on L-/M-cone excitation can be deduced from the derivative of Eq. (7):

$$\begin{aligned} \log(\Delta L_c) = {} & \log(L_{\text{th}}) - \log[G(L_A)/l_{\max} + G(M_A)/m_{\max}] \\ & + \log[(OPP_C + SAT)^2/SAT], \end{aligned} \tag{8}$$

where L_{th} represents $\delta/R_{\max}$, a vertical scaling factor. Therefore, L/M discrimination in the presence of one adapting field is determined by three terms: the first related to the criterion and static saturation, the second related to gain, and the third related to opponency [4,7,13]. There are two free parameters for this model, i.e., L_{th} and SAT.

B. Models for Two Adapting Fields

To model L/M chromatic discrimination with two adapting fields (A_1 with cone excitations of L_{A1} and M_{A1}, and A_2 with cone excitations of L_{A2} and M_{A2}), the model described in Eqs. (1)–(8) needs to be extended. We considered two model extensions that were dependent on different assumptions for how the contributions from the two adapting fields are combined. The first assumes that the spectral opponency signal is generated by the test cone excitations and weighted average of cone excitations from the two adapting fields. The second assumes that the test field generates spectral opponency separately in relation to each of the two adapting fields, with the resulting opponency signals subsequently combined.

Mathematically, the first model extension can be expressed as

$$L_{A1,2} = (\omega_1 L_{A1}^Q + \omega_2 L_{A2}^Q)^{1/Q}, \tag{9}$$

$$M_{A1,2} = (\omega_1 M_{A1}^Q + \omega_2 M_{A2}^Q)^{1/Q}, \tag{10}$$

where ω_1 and ω_2 are relative weights of A_1 and A_2 cone excitations, respectively, and Q is the quick-pooling parameter. Equations (9) and (10) are a more general form of cone excitation averaging. For instance, spatial averaging is a special case of Eqs. (9) and (10) with $Q = 1$ and ω_1 and ω_2 determined by spatial areas. The resulting weighted averages of L- and M-cone excitations from the two adapting fields are then fed into Eqs. (1) and (2), respectively. The remaining parts of the model are identical to Eqs. (3)–(8). This weighted averaging of cone excitations from the two adapting fields in the model is plausible, for example, if there were a large ganglion cell receptive field covering both adapting fields or if eye movements lead to spatial averaging. The summation of cone excitations would likely originate in the retina. For convenience, we refer to this model as a retinal summation model.

For the second model extension, spectral opponency signals are generated separately for the test and each of the two adapting fields

$$OPP_{C1} = OPP_T - k_4 OPP_{A1}, \tag{11}$$

$$OPP_{C2} = OPP_T - k_4 OPP_{A2}, \tag{12}$$

where OPP_{C1} and OPP_{C1} are opponency signals generated between the test and A_1 and between the test and A_2, respectively. Then the two opponency signals are pooled:

$$OPP_{C1,2} = (\omega_1 OPP_{C1}^Q + \omega_2 OPP_{C2}^Q)^{1/Q}, \tag{13}$$

where ω_1 and ω_2 are relative weights of two opponency signals, and Q is the quick-pooling parameter. Finally, the pooled opponency signal is subject to a chromatic contrast response:

$$R_{OPP1,2} = R_{\max} \cdot OPP_{C1,2}/(OPP_{C1,2} + SAT). \tag{14}$$

Because opponency between the test and each of the adapting fields is generated at the ganglion cell level, the summation of the two opponency signals needs to originate at a postretinal site. Anatomical studies have shown that, in primates, the number of lateral geniculate nucleus (LGN) neurons is similar to the number of ganglion cells, suggesting a nearly 1:1 projection from the ganglion cell level to the LGN [19]. In this sense, this model implies a cortical origin for the summing of the two opponency signals. For convenience, we refer to this model as a cortical summation model.

C. Model Fits

Chromatic discrimination data from control conditions with equivalent chromaticities in both adapting fields (i.e., red–red, white–white, and green–green pairs) were fitted using Eq. (8) with common parameters (L_{th} and SAT) for all three pairs. These two parameters (L_{th} and SAT) searched from the control conditions were then fixed when fitting the retinal

summation model or the cortical summation model to chromatic discrimination data in the presence of two different chromaticities in the two adapting fields, with a constraint that $\omega_1 + \omega_2 = 1$. Therefore, for each adapting field combination with different chromaticities (i.e., red–green, green–red, red–white, white–red, green–white, or white–green), both models had the same number of free parameters, that is, ω_1 and Q. The parameters were searched by minimizing the residual sum of squares. This analysis framework allowed us to infer whether the neural site mediating summing contributions from two different adapting fields was retinal or cortical and to estimate relative contributions of the two adapting fields to chromatic discrimination.

6. EXPERIMENT 1: FIXATION LOCATED IN THE CENTER OF THE INNER ADAPTING FIELD

A. Procedure

At the beginning of a session, observers dark adapted for 60 s. A session consisted of the presentation of one pair of adapting fields with six annulus chromaticities. For each annulus chromaticity, observers adapted for 30 s. L/M discrimination was measured using a spatial two-alternative forced choice (2AFC) random double staircase procedure, with one staircase for an increment and the other for a decrement in $L/(L+M)$. During each trial, the fan-shaped test patch was randomly presented to the left or right. The $L/(L+M)$ chromaticity change was presented in one cycle of a 1.5 s raised cosine window to minimize temporal transients or possible afterimages. Having a short duration would lead to a steep rising or declining slope in chromaticity change from the baseline to the peak or in the raised cosine window and may activate the magnocellular pathway [20]. This stimulus presentation method has been used in other studies on chromatic discrimination [4,5,13]. Observers were instructed to maintain fixation during a trial and to identify the location of the test by pressing buttons on a gamepad sensed by the computer. The staircase procedure continued until six reversals occurred for each staircase. The last four reversals were averaged and were considered as the threshold estimate. The staircase procedure was then repeated for another annulus chromaticity. Each session lasted about 20 min. Each session was repeated four times on different days. Increment and decrement discrimination thresholds were essentially the same, and the average was reported as the discrimination threshold.

B. Results

Figure 2A shows L/M discrimination thresholds for the adapting fields with equal chromaticities (red–red, white–white, and green–green pairs), expressed as log ΔL trolands as a function of annulus log L trolands. For the annulus chromaticities used in the study, the discrimination thresholds had a negative slope for the red–red pair, a V shape for the white–white pair, and a positive slope for the green–green pair, with minima occurring at the adapting chromaticities. These results confirmed the classical finding when using only one adapting field; that is, chromatic discrimination is best at the adapting chromaticity. The solid lines in Fig. 2 are model fits based on the model for one adapting field [Eqs. (1)–(6)] with a common criterion parameter (L_{th}) and half-saturation parameter (SAT) for all three equal-chromaticity pairs (for observer DC: $L_{\text{th}} = 0.998$; $SAT = 7.174$; for observer YL: $L_{\text{th}} = 1.600$, $SAT = 5.415$, also see Table 1 for the fitted parameter values).

Figures 2B, 2C, and 2D show the L/M discrimination thresholds when using two different adapting chromaticities. For the red–green pair (solid circles in Fig. 2B), discrimination thresholds as a function of annulus chromaticity had a negative slope with a minimum at the red chromaticity. This pattern was similar to the red–red pair (top row in Fig. 2), except the slope was shallower with the red–green pair, suggesting the inner adapting field (red) had more of an influence than the outer adapting field (green). Similarly, for the green–red pair, the discrimination pattern had a positive slope with a minimum at the green chromaticity. The pattern was similar to the green–green pair, except the slope was shallower than the green–green pair, suggesting the inner adapting field (green) weighted more in determining the threshold than the outer field (red).

Unlike the red–green and green–red pairs, in which discrimination thresholds depended more on the inner adapting field, the red–white and white–red pairs had almost identical discrimination patterns, with a minimum occurring near the white chromaticity (Fig. 2C). There were similar results for green–white and white–green pairs, with a minimum occurring near the white chromaticity (Fig. 2D).

The data for different adapting chromaticities (Fig. 2) were used to evaluate the retinal summation versus cortical summation models. The retinal summation model predicted a V-shape discrimination function, with the minimum occurring at a chromaticity between the two adapting chromaticities. With the relative weight of one adapting field increased (for instance, the red field in the red–green pair), the minimum shifted closer to the adapting chromaticity (red) in this model. However, the data in Fig. 2B did not show any minima between the two adapting chromaticities. If one of the relative weights was 0 or 1, that is, only one adapting field was affecting the chromatic discrimination, the retinal summation model predicts a slope comparable to that obtained with the equal-chromaticity pair, given the two parameters L_{th} and SAT are set to be identical to the equal-chromaticity pair. However, the red–green and green–red pairs had much shallower slopes than the red–red and green–green pairs. The retinal summation model as implemented has failed to account for the results (see Fig. 3 for the best fit of the retinal summation model for the discrimination thresholds with the red–green and green–red pairs).

In contrast, for the same condition, the cortical summation model could describe the data adequately (see solid lines in Fig. 3 and in Figs. 2B, 2C, and 2D). For each observer, the model fits used the same criterion (L_{th}) and saturation (SAT) values as those used for the two equal adapting chromaticity conditions. The model fits had a constraint that the sum of the inner field weight (ω_i) and outer field weight (ω_o) were equal to 1; i.e., $\omega_i + \omega_o = 1$. The log transformation of the weight ratio, $D = \log(\omega_i/\omega_o)$, can be considered as a dominance index, because if $D > 0$, then the inner adapting field dominates the outer field in determining chromatic discrimination, while if $D < 0$, then the outer field dominates. Table 1 lists the fitted parameters for the cortical summation model. Clearly, for the red–green, green–red, white–red, and white–green pairs, the inner adapting field dominated with the dominance index in the range of 0.558 to 1.147 for observer DC or 0.519 to 1.742 for observer YL. For the red–white and green–white pairs, the

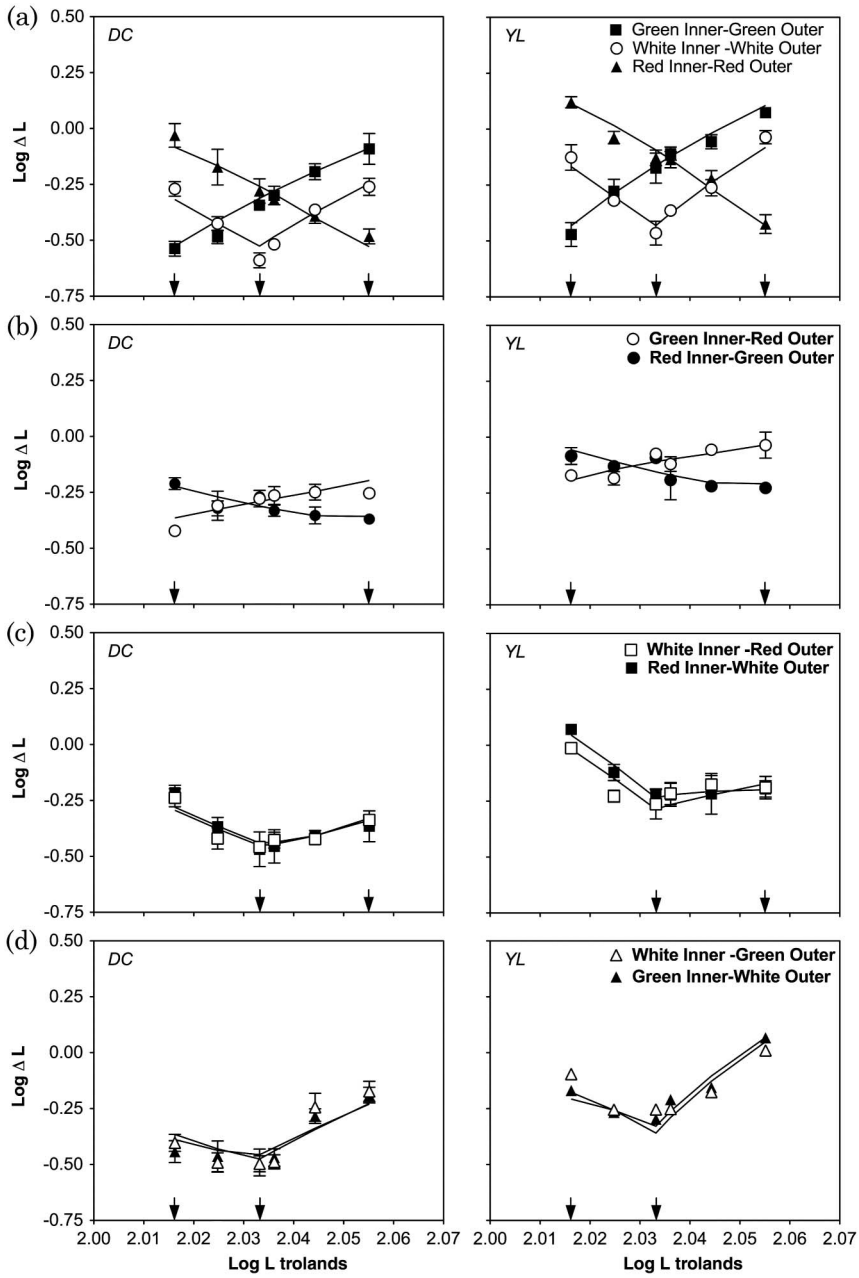

Fig. 2. L/M discrimination thresholds with the fixation located in the inner field, expressed as log ΔL trolands as a function of annulus log L trolands. A, red–red, white–white, and green–green pairs; B, red–green and green–red pairs; C, red–white and white–red pairs; D, green–white and white–green pairs. The arrows indicate the adapting chromaticities. The solid lines are fits from the PC-ganglion cell response based model with one adapting field for the control conditions (A) or from the cortical summation model for two adapting fields (B, C, and D).

outer adapting field dominated with dominance indices of −0.717 and −0.641 for DC or −0.185 and −0.41 for YL, respectively. The pooling parameter Q was in the range of 0.972 to 1.435 for DC and 0.772 to 1.285 for YL.

7. EXPERIMENT 2: FIXATION LOCATED IN THE OUTER ADAPTING FIELD

A. Procedure

Experiment 2 was the same as experiment 1 except that the fixation was set at the outer adapting field, 7° away from the test patch center, which was the same as the distance between the fixation and test patch center in experiment 1. For experiment 2, chromatic discrimination thresholds were measured using a temporal 2AFC double random staircase procedure. In each trial, the test appeared in one of two intervals, with a 0.5 s separation between the intervals. Each interval lasted for 1.5 s, with the L/(L + M) chromaticity change displayed in one cycle of a 1.5 s raised cosine envelope, as in experiment 1. Observers were instructed to maintain fixation during a trial. The task of the observers was to press buttons in the gamepad to indicate the interval of the chromaticity change.

B. Results

Figure 4 shows the chromatic discrimination thresholds with the fixation located at the outer adapting field. Chromatic discrimination thresholds for equivalent chromaticities in

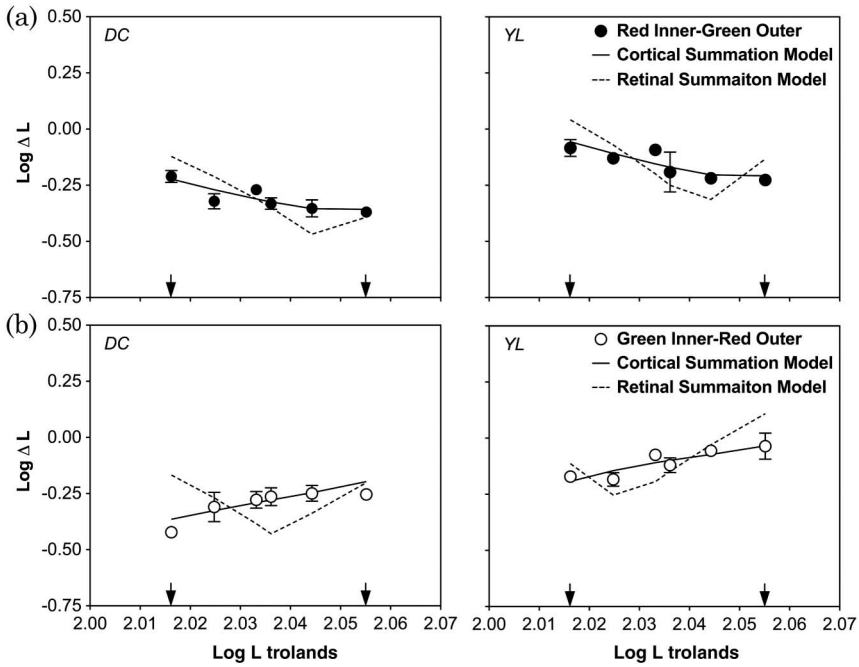

Fig. 3. Model fit comparison from the retinal summation and cortical summation models for the data from the red–green pair (A) and the green–red pair (B). The dashed lines are best fits from the retinal summation model. The solid lines are fits from the cortical summation model.

Table 1. Fitted Parameters for the Cortical Summation Model for Experiment 1 (Fixation in the Inner Field) and Experiment 2 (Fixation in the Outer Field)

Observer	Adapting Field Pairs	Fixation	Model Parameters: Criterion L_{th}	Saturation SAT	Weight (Inner) W_i	Weight (Outer) W_o	Dominance Index $D = \text{Log}(W_i/W_o)$	Pool Q
	Control conditions[a]	Inner	0.998	7.174	—	—	—	—
	Red–green	Inner	0.998	7.174	0.636	0.364	0.558	1.348
	Green–red	Inner	0.998	7.174	0.703	0.297	0.862	0.972
	Red–white	Inner	0.998	7.174	0.328	0.672	–0.717	1.365
	White–red	Inner	0.998	7.174	0.706	0.294	0.876	1.435
	Green–white	Inner	0.998	7.174	0.345	0.655	–0.641	1.263
	White–green	Inner	0.998	7.174	0.759	0.241	1.147	1.133
DC	Control conditions	Outer	1.059	5.481	—	—	—	—
	Red–green	Outer	1.059	5.481	0.249	0.751	–1.104	0.594
	Green–red	Outer	1.059	5.481	0.398	0.602	–0.414	0.653
	Red–white	Outer	1.059	5.481	0.163	0.837	–1.636	0.616
	White–red	Outer	1.059	5.481	0.639	0.361	0.571	0.703
	Green–white	Outer	1.059	5.481	0.212	0.788	–1.313	0.801
	White–green	Outer	1.059	5.481	0.771	0.229	1.214	0.826
	Control conditions	Inner	1.600	5.415	—	—	—	—
	Red–green	Inner	1.600	5.415	0.627	0.373	0.519	1.285
	Green–red	Inner	1.600	5.415	0.661	0.339	0.668	0.876
	Red–white	Inner	1.600	5.415	0.454	0.546	–0.185	0.772
	White–red	Inner	1.600	5.415	0.666	0.334	0.690	0.844
	Green–white	Inner	1.600	5.415	0.243	0.757	–1.134	0.703
	White–green	Inner	1.600	5.415	0.876	0.124	1.955	0.65
YL	Control conditions	Outer	2.394	4.145	—	—	—	—
	Red–green	Outer	2.394	4.145	0.286	0.714	–0.915	1.291
	Green–red	Outer	2.394	4.145	0.323	0.677	–0.740	0.890
	Red–white	Outer	2.394	4.145	0.360	0.640	–0.575	1.090
	White–red	Outer	2.394	4.145	0.530	0.470	0.120	0.759
	Green–white	Outer	2.394	4.145	0.340	0.660	–0.663	0.858
	White–green	Outer	2.394	4.145	0.543	0.457	0.172	0.850

[a]Control conditions are the adapting field pairs with equivalent chromaticities, including the red–red, white–white, and green–green pairs. A common criterion and saturation parameters were used for all of the conditions for each observer for each experiment.

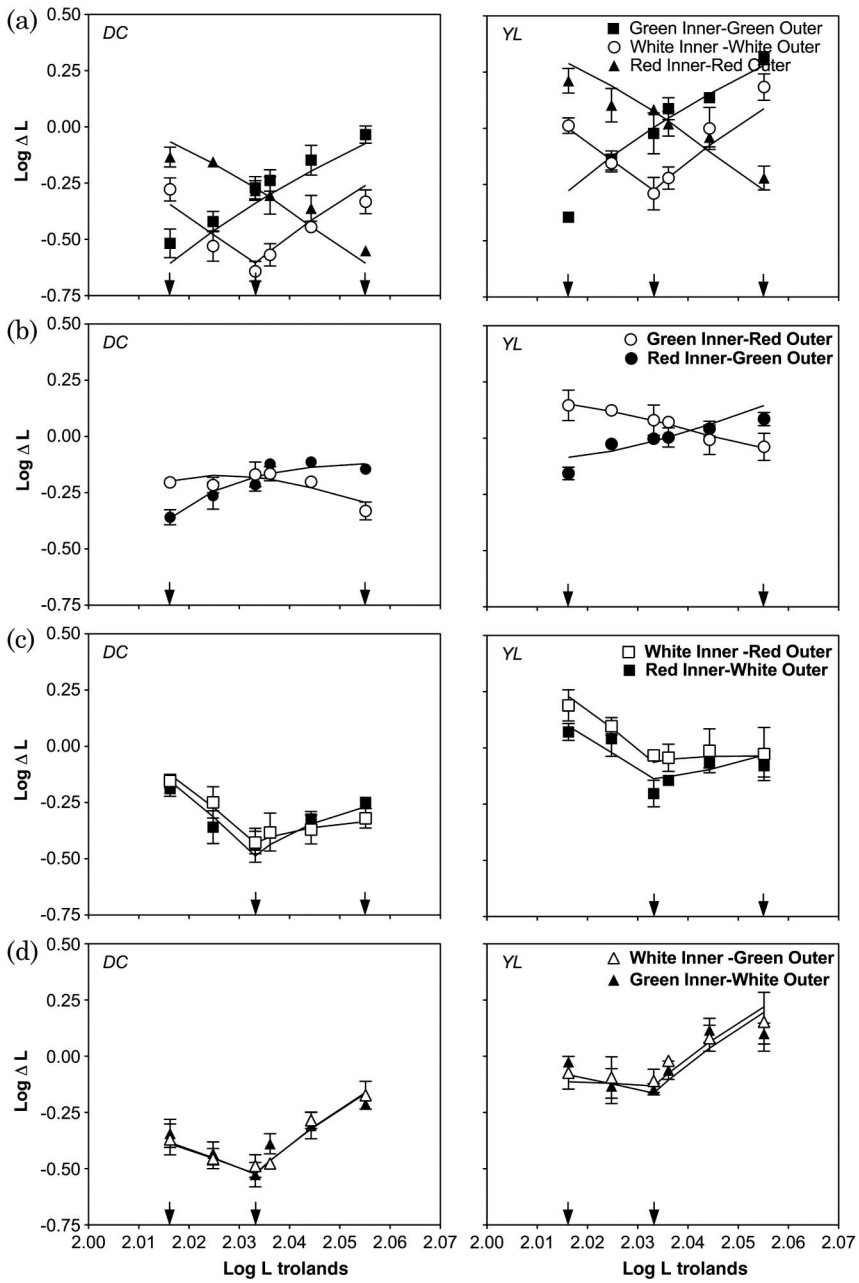

Fig. 4. L/M discrimination thresholds with the fixation located in the outer field (same format as Fig. 2).

the adapting fields had the same patterns as those with the same conditions in experiment 1 (see Figs. 2A and 3A). For the red–green or green–red pair, the change in fixation location changed the dominance of the adapting fields, with the outer field weighted more than the inner field (Fig. 3B). The model parameters with identical criterion and saturation values as the control conditions in experiment 2 are shown in Table 1. The dominance indices for the red–green and green–red pairs were negative ($D = -1.380$ and -0.494 for DC and -0.852 and -0.768 for YL, respectively), suggesting that the outer adapting field dominated the inner adapting field in determining discrimination thresholds. The pooling parameter was approximately 0.5–0.7 for both observers, which was slightly lower than those in experiment 1, probably due to the difference in the measurement methods (spatial 2AFC in experiment 1 and temporal 2AFC in experiment 2). On the other hand, when one of the adapting fields was white, the white field always dominated the contribution compared to another field (see Figs. 3B and 3C and Table 1 for model fits).

8. DISCUSSION

In this study, we measured L/M discrimination in the presence of two uniform adapting fields, with the fixation in the inner or outer field. For the pairs of adapting fields consisting of red and green, the inner field was weighted more than the outer field when the fixation was inside the inner field, but the outer field became dominant when the fixation was set in the outer field. When one of the adapting fields was white, however, the white field always dominated the other field, whether the

fixation was in the inner or outer field. These results implied that cortical mechanisms are involved in determining the relative contributions from the two adapting fields with different chromaticities. Of course, these findings might be dependent on our unique stimulus configuration. It is likely that a different spatial arrangement of two adapting fields would reveal a different summation pattern.

One common notion is that the signals generated along the edges between the test and adapting field determine discriminability, probably due to eye movements, and "the edge is all that matters" [4]. However, eye movements cannot explain the effects of fixation change on the inner–outer dominance for the red–green or green–red pair because, in both experiments, the stimuli were identical except for the fixation location. In the stimulus, the inner edge of the fan-shaped test patch was shorter than the outer edge. During the experiment, the observers were instructed to maintain fixation. It is unlikely that this different length would change the fixational eye movement pattern with a different fixation location. Therefore, whether the fixation was set in the inner or outer adapting field, the temporal variation would be similar along the border between the test and adapting fields generated by fixational eye movements. Of course, it is likely that the edge closer to the fixation point is sharper and therefore receives more weight than the other edge. However, visual neurons in V1 showed similar response properties whether an edge was sharp or blurred [21], ruling out the explanation based on the difference in sharpness between the two edges. Another possible explanation for this fixation location effect is that the fovea region, where fixation locates, has a larger cortical magnification factor than the periphery, because the ratio of the number of ganglion cell to cones is the highest in the fovea region but decreases in the periphery [22,23]. However, this cortical magnification interpretation cannot explain the dominance of a white adapting field, whether it was located inside or outside the test annulus. Another possible explanation for the fixation location effect is attentional variation. It is likely that the adapting field where fixation locates receives more attention and therefore more weight than the other field. Studies have shown that a concurrent chromatic attention task in the fovea improved chromatic discrimination [24]. However, again, this attention effect cannot explain the white field dominance when the white adapting field was outside the test annulus. It has been suggested that the visual system has an intrinsic representation of neutral color [25], resulting from some normalization processing to the lights in the natural environment [26]. Chromatic discrimination functions measured in a dark surround showed a V shape with a minimum at equal-energy-white, also suggesting intrinsic normalization toward equal-energy-white [4]. This intrinsic representation of white may explain why the visual system assigns more weight to the white adapting field.

Chromatic discrimination in the presence of one adapting field can be explained by a retinal spectral processing model. To account for the effects of two adapting fields, the model was extended to consider either a retinal summation or cortical summation mechanism. The retinal summation model could not account for the results obtained in this study, while the cortical summation described the data adequately, implying a cortical mechanism in determining the relative contributions of the two adapting fields. In contrast, using a chromatic textured adaptation, Zaidi *et al.* [8] suggested that a worst detector model could explain their results, suggesting that the spatial configurations in the stimuli played an important role in chromatic adaptation. Apparently, for the adapting fields consisting of red and green, the worst detector model cannot explain our results. Suppose that the visual system adapts to the red or green field independently; the worst detector model would predict an inverse V-shaped discrimination function for the red–green pair or the green–red pair. On the other hand, the best detector model would predict a V-shaped function. None of these patterns were observed in our results, ruling out the interpretation of the best or worst detector model. The cortical summation model assumed two spectral opponency signals from the test, and the two adapting fields were generated and then combined. In a parafoveal chromatic discrimination task, Danilova and Mollon [27–29] showed that discriminating two patches did not depend on the distance between them, which also suggested that a cortical mechanism compared the chromatic signal from each of the patches. Considering their results and our data, it is likely that separate spectral signals are generated from the different fields, and they then feed into the cortex for further processing.

ACKNOWLEDGMENTS

This study was supported by a National Institutes of Health (NIH) NEI grant R01 019651 (Cao, D.). We thank Drs. Joel Pokorny and Margaret Lutze for their comments on this manuscript.

REFERENCES

1. D. I. A. MacLeod and R. M. Boynton, "Chromaticity diagram showing cone excitation by stimuli of equal luminance," J. Opt. Soc. Am. **69**, 1183–1185 (1979).
2. R. M. Boynton and N. Kambe, "Chromatic difference steps of moderate size measured along theoretically critical axes," Color Res. Appl. **5**, 13–23 (1980).
3. Q. Zaidi, A. Shapiro, and D. Hood, "The effect of adaptation on the differential sensitivity of the S-cone color system," Vision Res. **32**, 1297–1318 (1992).
4. V. C. Smith, J. Pokorny, and H. Sun, "Chromatic contrast discrimination: data and prediction for stimuli varying in L and M cone excitation," Color Res. Appl. **25**, 105–115 (2000).
5. D. Cao, A. J. Zele, V. C. Smith, and J. Pokorny, "S-cone discrimination for stimuli with spatial and temporal chromatic contrast," Vis. Neurosci. **25**, 349–354 (2008).
6. J. Krauskopf and K. Gegenfurtner, "Color discrimination and adaptation," Vision Res. **32**, 2165–2175 (1992).
7. J. Pokorny and V. C. Smith, "Chromatic discrimination," in *The Visual Neurosciences*, L. M. Chalupa and J. S. Werner, eds. (MIT, 2004), pp. 908–923.
8. Q. Zaidi, B. Spehar, and J. DeBonet, "Adaptation to textured chromatic fields," J. Opt. Soc. Am. A **15**, 23–32 (1998).
9. M. D. Fairchild and P. Lennie, "Chromatic adaptation to natural and incandescent illuminants," Vision Res. **32**, 2077–2085 (1992).
10. A. Li and P. Lennie, "Mechanisms underlying segmentation of colored textures," Vision Res. **37**, 83–97 (1997).
11. T. Hansen, M. Giesel, and K. R. Gegenfurtner, "Chromatic discrimination of natural objects," J. Vision **8** (1), 2 (2008).
12. M. Giesel, T. Hansen, and K. R. Gegenfurtner, "The discrimination of chromatic textures," J. Vision **9** (9), 11 (2009).
13. A. J. Zele, V. C. Smith, and J. Pokorny, "Spatial and temporal chromatic contrast: effect on chromatic contrast discrimination for stimuli varying in L- and M-cone excitation," Vis. Neurosci. **23**, 495–501 (2006).
14. Y. Le Grand, *Light, Colour and Vision*, 2nd ed. (Chapman & Hall, 1968).

15. V. C. Smith and J. Pokorny, "The design and use of a cone chromaticity space," Color Res. Appl. **21**, 375–383 (1996).
16. V. C. Smith and J. Pokorny, "Spectral sensitivity of the foveal cone photopigments between 400 and 500 nm," Vision Res. **15**, 161–171 (1975).
17. V. C. Smith, B. B. Lee, J. Pokorny, P. R. Martin, and A. Valberg, "Responses of macaque ganglion cells to the relative phase of heterochromatically modulated lights," J. Physiol. **458**, 191–221 (1992).
18. B. B. Lee, J. Pokorny, V. C. Smith, and J. Kremers, "Responses to pulses and sinusoids in macaque ganglion cells," Vision Res. **34**, 3081–3096 (1994).
19. P. D. Spear, C. B. Y. Kim, A. Ahmad, and B. W. Tom, "Relationship between numbers of retinal ganglion cells and lateral geniculate neurons in the rhesus monkey," Vis. Neurosci. **13**, 199–203 (1996).
20. J. Pokorny, V. C. Smith, B. B. Lee, and T. Yeh, "Temporal sensitivity of macaque ganglion cells to lights of different chromaticities," Color Res. Appl. **26**, S140–S144 (2001).
21. M. L. Risner and T. J. Gawne, "The response dynamics of primate visual cortical neurons to simulated optical blur," Vis. Neurosci. **26**, 411–420 (2009).
22. H. Wässle, U. Grünert, J. Röhrenbeck, and B. B. Boycott, "Cortical magnification factor and the ganglion cell density of the primate retina," Nature **341**, 643–646 (1989).
23. H. Wässle, U. Grünert, J. Röhrenbeck, and B. B. Boycott, "Retinal ganglion cell density and cortical magnification factor in the primate," Vision Res. **30**, 1897–1911 (1990).
24. M. C. Morrone, V. Denti, and D. Spinelli, "Color and luminance contrasts attract independent attention," Curr. Biol. **12**, 1134–1137 (2002).
25. M. A. Webster and D. Leonard, "Adaptation and perceptual norms in color vision," J. Opt. Soc. Am. A **25**, 2817–2825 (2008).
26. J. Walraven and J. Werner, "The invariance of unique white; a possible implication for normalizing cone action spectra," Vision Res. **31**, 2185–2193 (1991).
27. M. V. Danilova and J. Mollon, "The comparison of spatially separated colours," Vision Res. **46**, 823–836 (2006).
28. M. Danilova and J. Mollon, "The gap effect is exaggerated in parafovea," Vis. Neurosci. **23**, 509–517 (2006).
29. M. V. Danilova and J. Mollon, "Parafoveal color discrimination: a chromaticity locus of enhanced discrimination," J. Vision **10** (1), 4 (2010).